Since January 2020 Elsevier has created a COVID-19 resource centre with free information in English and Mandarin on the novel coronavirus COVID-19. The COVID-19 resource centre is hosted on Elsevier Connect, the company's public news and information website.

Virology 378 (2008) 34–47

Contents lists available at ScienceDirect

Virology

journal homepage: www.elsevier.com/locate/yviro

A model for the dynamic nuclear/nucleolar/cytoplasmic trafficking of the porcine reproductive and respiratory syndrome virus (PRRSV) nucleocapsid protein based on live cell imaging

Jae-Hwan You [a], Gareth Howell [a], Asit K. Pattnaik [b], Fernando A. Osorio [b], Julian A. Hiscox [a,c,*]

[a] Institute of Molecular and Cellular Biology, Faculty of Biological Sciences, University of Leeds, Leeds, UK
[b] Nebraska Center for Virology, E249A Beadle, Lincoln, USA
[c] Astbury Centre for Structural Molecular Biology, University of Leeds, Leeds, UK

ARTICLE INFO

Article history:
Received 8 February 2008
Returned to author for revision
7 March 2008
Accepted 19 April 2008
Available online 12 June 2008

Keywords:
Nuclear export
Nuclear import
PRRSV
Nucleocapsid protein
Nucleolus
Nucleus
Cytoplasm
Confocal
FLIP
FRAP
Arterivirus
Virus
Nucleolar

ABSTRACT

Porcine reproductive and respiratory syndrome virus (PRRSV), an arterivirus, in common with many other positive strand RNA viruses, encodes a nucleocapsid (N) protein which can localise not only to the cytoplasm but also to the nucleolus in virus-infected cells and cells over-expressing N protein. The dynamic trafficking of positive strand RNA virus nucleocapsid proteins and PRRSV N protein in particular between the cytoplasm and nucleolus is unknown. In this study live imaging of permissive and non-permissive cell lines, in conjunction with photo-bleaching (FRAP and FLIP), was used to investigate the trafficking of fluorescent labeled (EGFP) PRRSV-N protein. The data indicated that EGFP-PRRSV-N protein was not permanently sequestered to the nucleolus and had equivalent mobility to cellular nucleolar proteins. Further the nuclear import of N protein appeared to occur faster than nuclear export, which may account for the observed relative distribution of N protein between the cytoplasm and the nucleolus.

Introduction

Porcine reproductive and respiratory syndrome virus (PRRSV) is a spherical, enveloped virus, which causes highly contagious, severe disease in the natural host, the swine, with a spectrum of disease states ranging from respiratory failure in neonates to abortions in sows and persistence (Wills et al., 2003). PRRSV is endemic to most swine producing countries and imposes a heavy economic burden due to the high mortality associated with the disease.

PRRSV is a positive strand RNA virus belonging to the *Arteriviridae* family, order *Nidovirales*. Although the primary site of replication is the cytoplasm, the viral encoded nucleocapsid (N) protein (an RNA binding protein) localises predominately in the cytoplasm and nucleolus during virus infection and when over-expressed in cell culture (Rowland et al., 1999). This property is common with related viruses including the equine arterivirus (EAV) N protein (Tijms et al., 2002) and the coronavirus N proteins (Hiscox et al., 2001; Wurm et al., 2001) with the possible exception of the severe acute respiratory syndrome coronavirus (SARS-CoV) N protein (Li et al., 2005; Rowland et al., 2005; Timani et al., 2005; You et al., 2005; You et al., 2007). Localisation and trafficking of the avian coronavirus infectious bronchitis virus (IBV) N protein to the nucleolus (Cawood et al., 2007) correlates with the stage in the cell cycle (G2) when virus protein synthesis and progeny virus production is most efficient (Dove et al., 2006; Harrison et al., 2007; Li et al., 2007).

The nucleolus is a dynamic sub-nuclear compartment found principally during interphase in eukaryotic cells (Andersen et al., 2005; Boisvert et al., 2007; Hernandez-Verdun, 2006; Matthews and Olson, 2006). Solution of the nucleolar proteome (Andersen et al., 2002) has indicated that the nucleolus has a number of functions ranging from ribosome subunit biogenesis to non-classical functions such as the stress response (Mayer and Grummt, 2005; Rubbi and Milner, 2003) and regulation of cell growth (Hernandez-Verdun and Roussel, 2003).

* Corresponding author. Institute of Molecular and Cellular Biology, Faculty of Biology Sciences, Garstang Building, University of Leeds, Leeds, LS2 6JT, England, UK. Fax: +44 1133433167.
E-mail address: j.a.hiscox@leeds.ac.uk (J.A. Hiscox).

0042-6822/$ – see front matter © 2008 Elsevier Inc. All rights reserved.
doi:10.1016/j.virol.2008.04.037

There are over 700 proteins associated with the nucleolar proteome (Leung et al., 2006) and these include nucleolin, fibrillarin and B23.1.

Localisation of positive strand RNA virus capsid proteins and replication proteins (and in one case partial RNA synthesis) in the nucleus and/or nucleolus appears to be an emerging feature of positive strand RNA viruses. The reason why positive strand RNA virus capsid proteins localise to the nucleolus is unknown, and several hypotheses have been proposed including; as part of a cellular defense mechanism to sequester viral proteins away from sites of virus replication and assembly, to recruit nucleolar proteins to facilitate virus replication, to usurp cellular processes by disrupting the nucleolar proteome or because the viral protein contains motifs which mimic nucleolar localisation signals (NoLSs) (Hiscox, 2002, 2003, 2007; Rowland and Yoo, 2003; Uchil et al., 2006; Weidman et al., 2003).

However, the majority of RNA synthesis in positive strand RNA viruses (Ahlquist, 2006; de Haan and Reggiori, 2008; Taylor and Kirkegaard, 2008) including arteriviruses (Posthuma et al., 2008; van Hemert et al., in press) is thought to occur on cytoplasmic membrane bound replication complexes. Assembly also occurs in the cytoplasm; therefore capsid proteins are required in this cellular compartment to facilitate these processes. This would infer the need for appropriate trafficking signals to ensure import and export from the nucleus and several such motifs have been identified. Mutational analysis and abrogation of nuclear/nucleolar localisation of viral proteins for the PRRSV N protein (Lee et al., 2006; Pei et al., 2008) and the positive strand RNA plant RNA virus groundnut rosette virus ORF3 (Kim et al., 2007a,b) have elegantly demonstrated the importance of nucleolar localisation in the biology of these viruses.

For PRRSV N protein, the motifs which direct nucleolar localisation are composed of a nuclear localisation signal (NLS) acting in concert with a NoLS (Lee et al., 2006; Rowland et al., 2003). Whereas for IBV N protein an eight amino acid motif was shown to be necessary and sufficient to act as an NoLS (Reed et al., 2006). For nuclear export of the arterivirus and coronavirus N proteins, nuclear export signals (NESs) have either been identified or inferred from molecular genetic and/or bioinformatic analysis, structural modeling or use of specific metabolic inhibitors of nuclear export (Reed et al., 2007; Rowland and Yoo, 2003; Tijms et al., 2002; You et al., 2007).

The dynamic trafficking of positive strand RNA virus capsid proteins between the nucleolus and the cytoplasm or the mobility in the nucleolus is not clearly understood. Previous studies which have been mainly based on preparations of fixed cells could not distinguish whether there were for example two populations of capsid protein; one which sequestered to the cytoplasm and one which sequestered to the nucleolus or whether protein trafficked between the two compartments. In order to distinguish between these possibilities and derive a model for PRRSV N protein trafficking, this study used live cell confocal microscopy to investigate the trafficking of fluorescent labeled N protein in porcine and non-porcine cell lines which were permissive and non-permissive for PRRSV.

Results and discussion

To investigate whether the localisation of N protein within live cells was equivalent to that previously observed in fixed cells and for subsequent trafficking analysis, the PRRSV *N* gene was PCR cloned downstream of the enhanced green fluorescent protein (EGFP) in the expression vector pEGFPC2. This created plasmid pEGFP-PRRSV-N, which when transfected into cells led to the expression of PRRSV N protein fused to EGFP. Although several cell lines were used in this study, primarily, the continuous porcine monocytic cell line, 3D4/31, was used in the majority of experiments. Although not permissive for PRRSV infection, these cells were derived from porcine alveolar macrophages (which are permissive) following expressing of the SV40 large T antigen (Weingartl et al., 2002).

To investigate the localisation of EGFP-PRRSV-N protein, 3D4/31 cells were co-transfected with pEGFP-PRRSV-N and a vector which directed the expression of the nucleolar protein B23.1 fused to DsRed (DsRed-B23.1) (Reed et al., 2006; You et al., 2005) to act as a marker for the nucleolus (Fig. 1A). Two different localisation patterns of EGFP-PRRSV-N protein were observed: In 3D4/31 cells which expressed lower amounts of EGFP-PRRSV-N protein, localisation was predominately nucleolar with some nuclear signal (Fig. 1A, panel A). In 3D4/31 cells which expressed higher amounts of protein localisation was predominately either cytoplasmic and nucleolar (Fig. 1A, panel C) or predominately nucleolar with some cytoplasmic and nuclear signal (Fig. 1A, panel D). This difference in expression was evident in that the fluorescent signal from EGFP-PRRSV-N protein in Fig. 1A, panel A was captured in the linear range. However, using the same setting led to over-saturated pixels in cells expressing higher amounts of EGFP-PRRSV-N protein e.g. Fig. 1A, panel B (red indicates that the image range is not linear). Gain adjustment to ensure pixels were captured in the linear range restored image clarity (Fig. 1A, panel C). Nucleolar localisation of EGFP-PRRSV-N protein was confirmed due to co-localisation with the nucleolar marker protein DsRed-B23.1 (yellow signal). Previously, N protein has been shown to interact with the nucleolar protein fibrillarin (Yoo et al., 2003).

There are several different mechanisms which may account for the concentration dependent localisation pattern of N protein. N protein could diffuse and/or be actively transported into the nucleus through the nuclear pore complex (NPC), diffuse through the nucleoplasm and be permanently sequestered in the nucleolus. As the nucleolar concentration of N protein becomes saturating so excess protein could either diffuse or be actively transported through the NPC to the cytoplasm. Alternatively, N protein could be continuously exchanged between the nucleolus and the nucleus and the cytoplasm, with localisation being driven by possible differential relative trafficking rates between nuclear import and export. To investigate and discriminate between these possibilities dynamic live cell imaging using fluorescence loss in photo-bleaching (FLIP) and fluorescence recovery after photo-bleaching (FRAP) was used to study movement of EGFP-PRRSV-N protein.

Relative trafficking within the nucleolus and trafficking from the cytoplasm to the nucleolus was investigated using FLIP to continuously photo-bleach a defined portion of the nucleolus in 3D4/31 cells expressing EGFP-PRRSV-N protein. This was compared to the trafficking of three nucleolar marker proteins (Reed et al., 2006; You et al., 2005); EGFP-nucleolin, EGFP-B23.1 and EFP-fibrillarin (Fig. 1B). Loss of fluorescence is then a result of the EGFP-tagged fusion protein trafficking into and out of the photo-bleached area with time. The data indicated that by 180s, loss of fluorescence from cells expressing EGFP-nucleolin and EGFP-fibrillarin was greater than EGFP-B23.1. In cells expressing lower amounts of EGFP-PRRSV-N protein, fluorescence was completely photo-bleached by 120s and in higher expressing cells EGFP-PRRSV-N protein fluorescence was completely photo-bleached in the nucleus and reduced in the cytoplasm by 180s (Fig. 1B). This indicated that PRRSV N protein was potentially as mobile as the cellular nucleolar proteins examined.

To compare the relative nucleolar mobility between EGFP-PRRSV-N protein and EGFP-nucleolin, EGFP-B23.1 and EFP-fibrillarin in 3D4/31 cells, FRAP was used to photo-bleach a defined portion of the nucleolus (Fig. 2A) and the time taken to refill the photo-bleached area was measured (Fig. 2B) and $t_{1/2}$ values were compared (Fig. 2C). The data indicated that EGFP-PRRSV-N protein had the lowest $t_{1/2}$ value and therefore had a slightly faster mobility than the three cellular nucleolar marker proteins used in this study. Cellular nucleolar proteins can have different mobility rates and nucleolar localisation patterns depending on their functions (Andersen et al., 2005) and can show a continuous rapid turn over between the nucleus and the nucleolus — yet the overall structure of the nucleolus is maintained (Misteli, 2001). The diffusion coefficient (D) value of EGFP-PRRSV-N protein and EGFP-nucleolin, EGFP-B23.1 and EFP-fibrillarin was

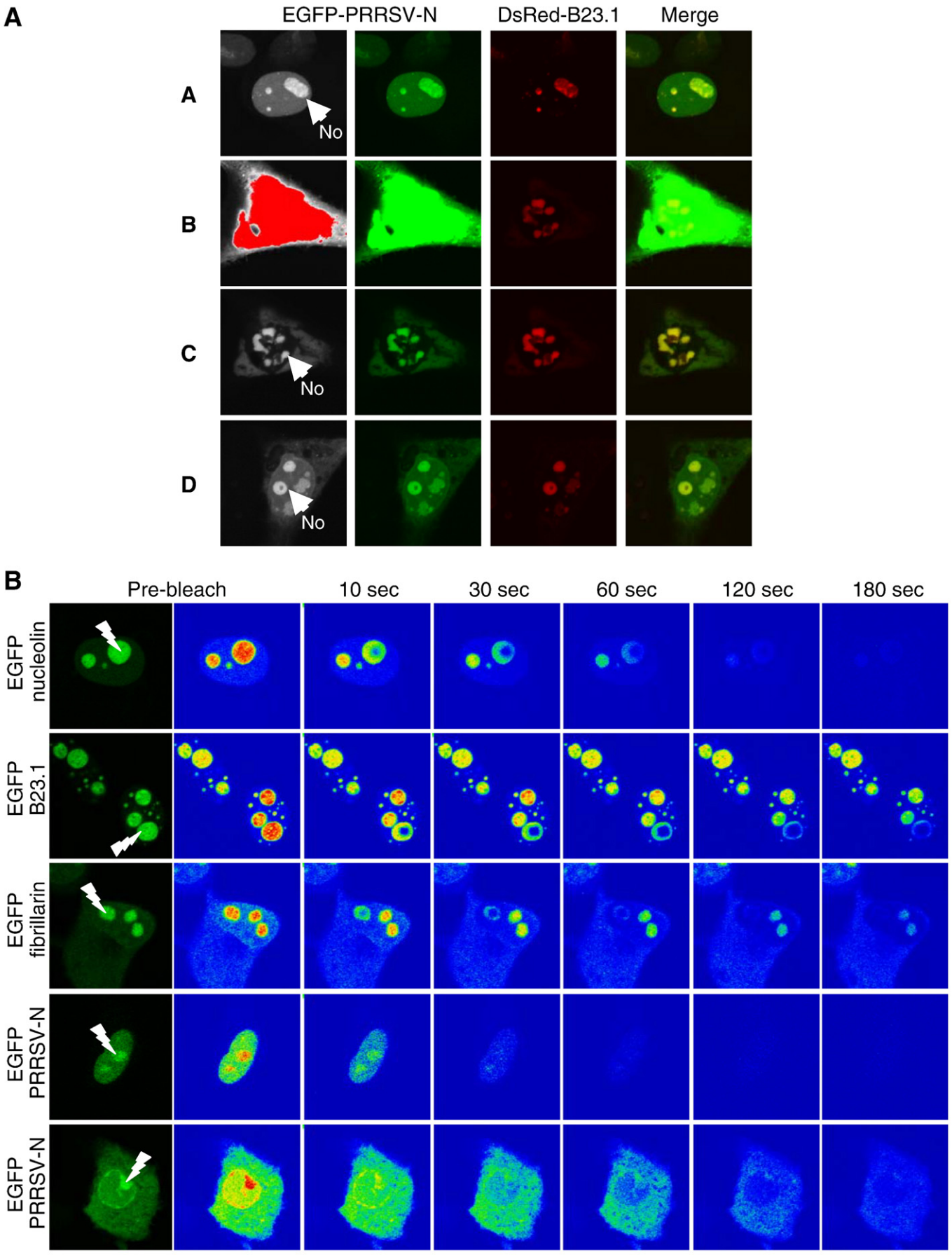
A
EGFP-PRRSV-N
DsRed-B23.1
Merge
A
B
C
D
No
No
No
B
Pre-bleach
10 sec
30 sec
60 sec
120 sec
180 sec
EGFP nucleolin
EGFP B23.1
EGFP fibrillarin
EGFP PRRSV-N
EGFP PRRSV-N

calculated from the recovery curves (Phair and Misteli, 2000). This value is the rate at which a protein repopulates a photo-bleached area. This confirmed that EGFP-PRRSV-N protein had an equivalent (or slightly higher) mobility (D=0.839 $\mu m^2/s$) than EGFP-nucleolin (D=0.156$\mu m^2/s$), EGFP-fibrillarin (D=0.278$\mu m^2/s$) or EGFP-B23.1 (D=0.166$\mu m^2/s$). In a previous study the half time of EGFP-fibrillarin in BHK cells was reported to be approximately 3s with a D value of 0.53$\mu m^2/s$ (Phair and Misteli, 2000), which is in similar agreement to this study. Phair and Misteli (2000) noted that the D values of EGFP-fibrillarin and other fluorescent tagged nuclear/nucleolar proteins were 100 times lower than that reported for free solutes in the nucleus and suggested that this was due to interactions with other nuclear components. Therefore, similar to the cellular nucleolar proteins the mobility of EGFP-PRRSV-N protein indicated that N protein probably localised to the nucleolus by diffusing through the nucleoplasm until it located an appropriate binding site, possibly a nucleolar protein or ribosomal RNA, and thus appeared to accumulate in this compartment. PRRSV N protein has been shown to interact with fibrillarin (Yoo et al., 2003).

The precise mechanism of trafficking of N protein within a cell and to the nucleolus is unknown, although N protein has been shown to interact with and pull down fibrillarin and thus may potentially localise to the nucleolus via this interaction (Yoo et al., 2003). For example, the nucleolin binding activity of hepatitis delta antigen is associated with nucleolar localisation (Ning and Shih, 2004). PRRSV N protein has also been shown to interact with importin-α and importin-β (Rowland et al., 2003) and is sensitive to leptomycin B (LMB), an inhibitor of CRM1-dependent export (Rowland and Yoo, 2003). Several different nuclear-cytoplasmic trafficking pathways are utilized by viruses (Whittaker et al., 2000) and have been described for a number of different virus nucleocapsids and nucleocapsid proteins. For example, in vesicular stomatitis virus nucleocapsids are trafficked via a microtubule mediated process (Das et al., 2006), as are the Hantaan virus nucleocapsid protein (Ramanathan et al., 2007) and the West Nile virus capsid protein (Chu and Ng, 2002). To investigate whether the trafficking of N protein between the cytoplasm and the nucleus/nucleolus was associated with microtubules or energy dependent, the mobility of EGFP-PRRSV-N protein was compared in 3D4/31 cells incubated at 37°C in the presence and absence of nocodazole (60ng/ml nocodazole (Sigma) for 16h), a microtubule inhibitor, or incubated at 10°C. In preparations of fixed cells, in the absence of nocodazole (Fig. 3A) microtubules were visualized (observed as filaments) using an anti-tubulin antibody. As before EGFP-PRRSV-N protein localised predominately to the nucleolus. In preparations of fixed cells in the presence of nocodazole (Fig. 3B) microtubule polymerization was inhibited (diffuse staining of tubulin), although similar to untreated cells, EGFP-PRRSV-N protein remained predominately localised in the nucleolus. The activity of nocodazole was also confirmed by analyzing the cell cycle stage of treated cells (using flow cytometry as described previously (Dove et al., 2006; Harrison et al., 2007)), which demonstrated enrichment in the G2/M stage (Fig. 3B) compared to untreated cells (Fig. 3A), and is a result of the inhibition of spindle formation in metaphase. To investigate the trafficking of EGFP-PRRSV-N protein in live cells, a nucleolus in 3D4/31 cells expressing EGFP-PRRSV-N protein was continuously photo-bleached (FLIP) in the presence of nocodazole at 37°C (Fig. 3C) and in the absence of nocodazole in cells that had been pre-cooled to 10°C (Fig. 3D). In both cases, photo-bleaching resulted in the loss of fluorescent signal in both the cytoplasm (where appropriate) and nucleus and the non photo-bleached nucleolus, indicating that cytoplasmic to nuclear trafficking occurred, and was not inhibited by either the presence of nocodazole or cooling to 10°C. This suggested that the trafficking of N protein from the cytoplasm to the nucleus was not microtubule or energy dependent. To investigate trafficking within the nucleolus a defined portion of the nucleolus was photo-bleached (FRAP) in cells incubated at either 37°C, 10°C or 37°C in the presence of nocodazole (Fig. 4A) and the time taken to refill the photo-bleached area was measured (Fig. 4B). The data indicated that EGFP-PRRSV-N protein at 37°C had a $t_{1/2}$ value of 0.74±0.07 which was similar to the $t_{1/2}$ value (0.75±0.18) at 4°C and at 37°C in the presence of nocodazole ($t_{1/2}$ value of 1.37±0.55).

The mobility of EGFP-PRRSV-N protein between the nucleolus and the cytoplasm and *vice versa* was compared to EGFP using FRAP and FLIP on the cytoplasm or the nucleus/nucleolus in 3D4/31 cells. EGFP is approximately 27kDa and contains no known NLS, NoLS or NES motifs and therefore the relative localisation of EGFP between the nucleus and the cytoplasm would reflect the relative trafficking of the protein across the NPC, most likely due to diffusion and concentration gradients, such that equilibrium would be reached depending on the relative balance between the rate of nuclear import versus nuclear export and the relative volume of the cytoplasm versus the nucleus. PRRSV N protein is approximately 15kDa (and with the addition of EGFP approximately 42kDa) and although the fusion protein has the potential to freely diffuse through the NPC (which has a size exclusion limit for passive transport of approximately 50kDa (Macara, 2001; Terry et al., 2007)), clearly EGFP-PRRSV-N protein has a discrete localisation pattern being cytoplasmic and nucleolar (with some nuclear signal) (Rowland et al., 1999). Without the presence of trafficking signals N protein would be predicted to display similar trafficking and localisation to EGFP.

The trafficking of EGFP compared to EGFP-PRRSV-N protein between the nucleus and the cytoplasm and *vice versa* was analyzed by FRAP (Fig. 5) and the relative level of fluorescence between the nucleus and the cytoplasm was measured using ImageJ software (NIH) as described (Reed et al., 2007) for the 3D4/31 cell line. This takes into account the reduction in fluorescence during photo-bleaching due to ongoing trafficking into and out of the bleach area. In EGFP-expressing 3D4/31 cells the pre-bleach level of EGFP in the nucleus to that of the cytoplasm was 0.56±0.05 to 0.44±0.03, respectively. To examine trafficking into the nucleus, this area was photo-bleached and subsequent recovery of fluorescence in the nucleus (due to import of EGFP from the cytoplasm) indicated that after 180s the relative level of EGFP between the nucleus and the cytoplasm was 0.60±0.04 compared to 0.41±0.05, respectively, which was not significantly different from the pre-bleach levels (Fig. 5A). Analysis by 180s was then used as a base line for comparison of trafficking of EGFP and EGFP-PRRSV-N protein between the nucleus and the cytoplasm in FRAP analysis. In 3D4/31 cells expressing EGFP-PPRSV-N protein with nucleolar/nuclear and cytoplasmic distribution, the pre-bleach level of EGFP-PRRSV-N protein between the total nuclear content and the cytoplasm was 0.78±0.07 and 0.22±0.03, respectively. 180s after photo-bleaching, the nuclear to cytoplasm level was 0.81±0.08 to 0.24±0.04, respectively (Fig. 5B), which was not significantly different from the pre-bleach level.

To examine trafficking of EGFP into the cytoplasm, this area was photo-bleached in 3D4/31 cells and subsequent recovery of fluorescence in the cytoplasm (due to import of non photo-bleached EGFP from the

Fig. 1. A. (Panels A, C and D). Live cell confocal microscope images of 3D4/31 cells showing different examples of the distribution of EGFP-PRRSV-N (green) and DsRed-B23.1 (red). Merged and transmission phase images are also presented. Co-localisation when it occurs is shown in yellow. Panel B is the range indicator for the fluorescent signal of EGFP-PRRSV-N and DsRed-B23.1 shown in panel A, for left most images red represents saturated pixels. For orientation an example of a nucleolus is indicated (No). (B). Comparison of trafficking analysis using FLIP to photo-bleach the nucleolus (arrowed) between three cellular nucleolar proteins tagged with EGFP; EGFP-nucleolin, EGFP-B23.1 and EGFP-fibrillarin with two examples of EGFP-PRRSV-N protein. Presented are the EGFP-protein signals to the left and then the corresponding rainbow image of this where regions of high protein concentration are denoted in red and low to no concentration in blue. Images were sampled after 10, 30, 60, 120 and 180 s of photo-bleaching. The position of the photo-bleach on the nucleolus is indicated by the tip of the lighting symbol. The width of all images is 35 μm.

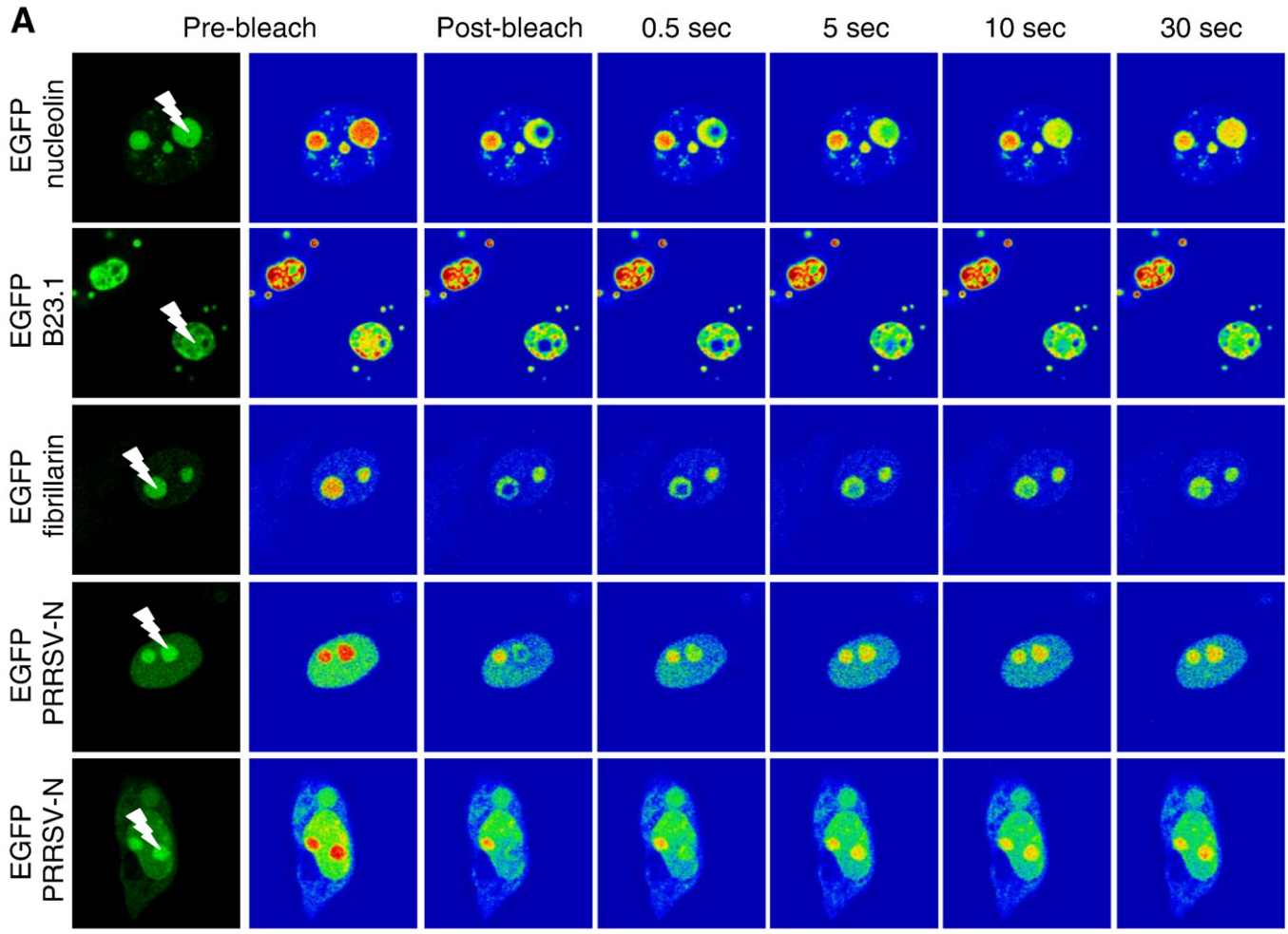
A
Pre-bleach
Post-bleach
0.5 sec
5 sec
10 sec
30 sec
EGFP nucleolin
EGFP B23.1
EGFP fibrillarin
EGFP PRRSV-N
EGFP PRRSV-N

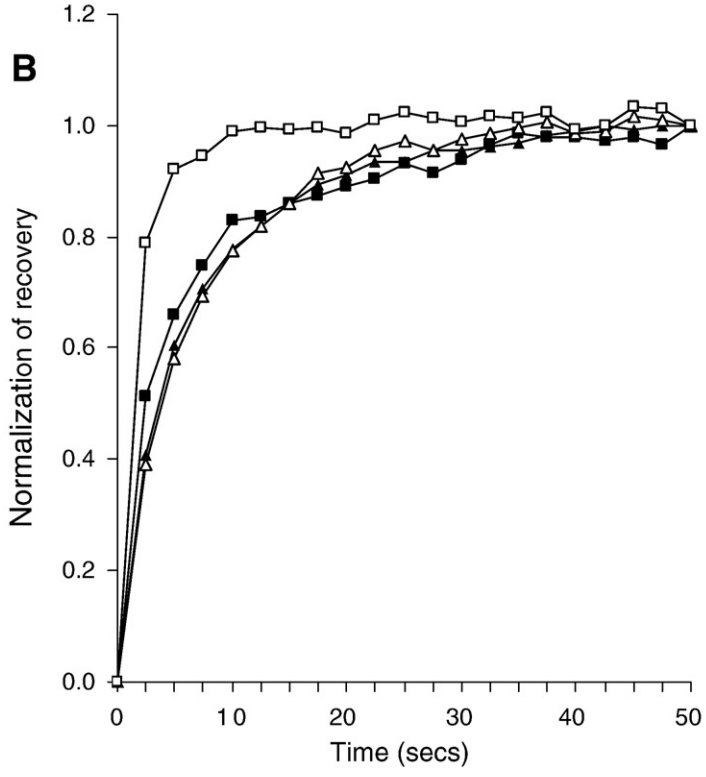
B
Normalization of recovery
Time (secs)
0.0
0.2
0.4
0.6
0.8
1.0
1.2
0
10
20
30
40
50

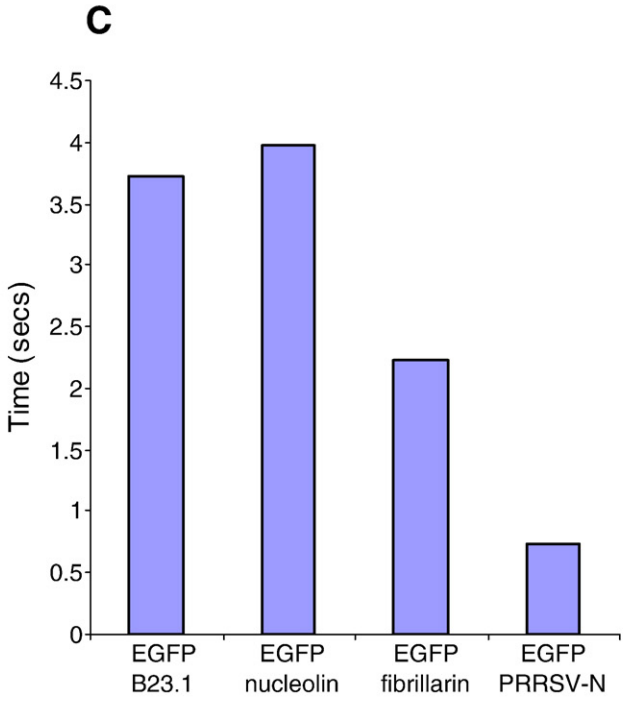
C
Time (secs)
0
0.5
1
1.5
2
2.5
3
3.5
4
4.5
EGFP B23.1
EGFP nucleolin
EGFP fibrillarin
EGFP PRRSV-N

nucleus) was compared to levels before photo-bleaching (nucleus to cytoplasm level of 0.58±0.04 to 0.41±0.05, respectively) to levels 180s after photo-bleach when the nuclear to cytoplasm ratio was 0.72±0.05 compared to 0.28±0.04, respectively (Fig. 5C). This indicated that EGFP had not reached pre-bleach levels, which was different when considering cytoplasm to nucleus trafficking.

To examine trafficking of EGFP-PRRSV-N protein into the cytoplasm, this area was photo-bleached and subsequent recovery of fluorescence in the cytoplasm (due to import of EGFP-PRRSV-N protein from the nucleus) was compared before photo-bleach (nucleus to cytoplasm relative level of 0.71±0.06 to 0.29±0.03, respectively) to 180s after photo-bleach, when the nuclear to cytoplasm ratio was 0.92±0.08 compared to 0.08±0.05, respectively (Fig. 5D). (Note that this experiment was performed on cells in which EGFP-PRRSV-N protein localised also in the cytoplasm). This data indicated that the ratio of EGFP-PRRSV-N protein had not reached pre-bleach levels, which was different when considering cytoplasm to nucleus trafficking. This indicated that the export of EGFP-PRRSV-N protein from the nucleus was potentially slower than import and given the difference in relative ratios, slower than the export of EGFP from the nucleus to the cytoplasm.

The relative difference between nuclear import and nuclear export observed with EGFP-PRRSV-N protein was investigated using FLIP in which either a defined area of the nucleus (not the nucleolus) was photo-bleached for either EGFP (Fig. 6A) or EGFP-PRRSV-N protein (Fig. 6B) expressing 3D4/31 cells or a defined area of the cytoplasm was photo-bleached for either EGFP (Fig. 6C) or EGFP-PRRSV-N protein (Fig. 6D) expressing 3D4/31 cells. Again, comparison of the data from the two proteins indicated that more fluorescent signal of EGFP-PRRSV-N protein was lost during import than export, suggesting that the former process operates faster than the latter. Reflecting the FRAP analysis, the relative trafficking of EGFP-PRRSV-N protein between the nucleus and the cytoplasm was in favor of nuclear import.

The observed live cell trafficking patterns of EGFP-PRRSV-N protein may have been specific to 3D4/31 cells. Therefore, to investigate this possibility, the localisation and dynamic trafficking of this protein was compared to EGFP in MARC-145 cells (an African green monkey kidney cell line permissive for PRRSV infection (Kim et al., 1993)) and HeLa cells (derived from a human cervical cell line, and non-permissive for infection). The data indicated that in both MARC-145 and HeLa cell types EGFP-PRRSV-N protein localised predominately to the nucleus/nucleolus compared to EGFP which localised throughout the cell (Figs. 7A and 8A, respectively). Very few cells (less than 5%) exhibited more than 10% of the total fluorescence from EGFP-PRRSV-N protein in the cytoplasm. Note that for EGFP, the transmission phase image is presented to highlight the differentiation between the cytoplasm, nucleus and nucleolus. (Such images were used in subsequent analysis for placement of photo-bleaching in the EGFP fluorescent cell, where distinction between the nucleus/nucleolus/cytoplasm was not possible). The sub-cellular localisation patterns for both fluorescent proteins were similar to that observed in 3D4/31 cells.

Investigation of the trafficking of EGFP-PRRSV-N protein compared to EGFP between the cytoplasm and the nucleus and *vice versa* by continuous photo-bleaching (FLIP) a defined portion of the nucleus or the cytoplasm in both MARC-145 cells (Fig. 7) and HeLa cells (Fig. 8), indicated that photo-bleaching in the nucleus in cells expressing EGFP resulted in apparent simultaneous loss of fluorescence from the nucleus and the cytoplasm (Figs. 7B and 8B), indicating rapid trafficking of EGFP between the two compartments. In comparison, little fluorescence (approximately ~5% of total fluorescence) of EGFP-PRRSV-N protein was observed in the cytoplasm in both MARC-145 and HeLa cells and photo-bleaching in the nucleus resulted in loss of fluorescence from the nucleoplasm and then the nucleolus (Figs. 7C and 8C upper panels, respectively). In approximately 10% of cells expressing EGFP-PRRSV-N protein fluorescence was observed in the cytoplasm, but only if imaging was adjusted so that the fluorescent signal in the nucleus/nucleolus was above the linear range (for example Fig. 8C, lower panels). In this case photo-bleaching in the nucleus resulted in loss of fluorescence from the cytoplasm which could be accounted by faster trafficking into the nucleus of non-photo-bleached protein which was then photo-bleached than the export of photo-bleached protein into the cytoplasm. Photo-bleaching in the cytoplasm of either MARC-145 cells or HeLa cells expressing EGFP resulted in loss of signal from both the nucleus and the cytoplasm (Figs. 7D and 8D, respectively). In comparison, photo-bleaching in the cytoplasm of either MARC-145 cells or HeLa cells expressing EGFP-PRRSV-N protein resulted in less loss of fluorescence when compared to EGFP (Figs. 7E and 8E). The photo-bleaching analysis for EGFP-PRRSV-N protein also indicated that when the nucleus was photo-bleached loss of fluorescence in the cytoplasm was due to the trafficking of non photo-bleached protein into the nucleus rather than the rapid export of photo-bleached protein from the nucleus into the cytoplasm. Thus the photo-bleaching analysis of EGFP and EGFP-PRRSV-N protein in MARC-145 and HeLa cells was similar to that found in 3D4/31 cells.

Thus we propose a model of N protein trafficking in which the nuclear import of N protein is faster than the nuclear export and N protein is apparently localised in greater amounts in the nucleolus (Fig. 9). The deficiency of the model is that the analysis was conducted in the absence of other viral proteins or RNA (i.e. infected cells) which may associate with N protein and alter its relative trafficking rates. This may be certainly true for the cytoplasm, where N protein will complex with viral RNA and possibly components of the replicase complex. Although there is currently no published data that other PRRSV macromolecules localise in the nucleus/nucleolus, the EAV non-structural protein 1 (nsp1) has also been observed in the nucleus (Tijms et al., 2002), and therefore PRRSV nsp1 may have similar properties. PRRSV N protein does not accumulate or is sequestered in the nucleus/nucleolus *per se* and in common with other cellular nuclear/nucleolar proteins is continuously being exchanged between the nucleolus and the nucleoplasm and indeed is as mobile as the cellular nucleolar proteins examined. The implication of this study is that all *de novo* synthesized N protein (when over-expressed) traffics to the nucleolus. Together with molecular genetic analysis showing that virus replication is reduced when N protein nucleolar localisation is abolished (Lee et al., 2006; Pei et al., 2008), suggests that the nucleolar trafficking of N protein is playing a crucial role in virus biology. What this role is remains to be elucidated.

Materials and methods

Cell culture

3D4/31 cells were grown at 37°C with 5% CO_2 in DMEM and RPMI 1640 (50:50). MARC-145 and HeLa cells were maintained in DMEM supplemented with 10% foetal bovine serum and grown at 37°C with 5% CO_2. 30mm glass bottom tissue culture dishes were seeded with 2×10^5 cells 24h prior to transfection.

Fig. 2. A. FRAP analysis of a defined portion of the nucleolus to compare the nucleolar trafficking of EGFP-nucleolin, EGFP-B23.1 and EGFP-fibrillarin with two examples of EGFP-PRRSV-N protein showing different distributions within a 3D4/31 cell. Presented are the EGFP-protein signals to the left and then the corresponding rainbow image of this where regions of high protein concentration are denoted in red and low to no concentration in blue. The pre- and post-bleach image for each fluorescent fusion protein is presented followed by images sampled at 0.5, 5, 10 and 30 s post-bleach. The width of all images is 35 μm. The position of the photo-bleach on the nucleolus is indicated by the tip of the lighting symbol. (B). Comparison of the normalization of recovery in the photo-bleached area of the nucleolus for EGFP-nucleolin (△), EGFP-B23.1, (▲) EGFP-fibrillarin (■) and EGFP-PRRSV-N protein (□) where data was processed to ensure the recovery profiles were set to zero at the initial time point post bleaching, and set to 1 at the final time point. (C) Comparison of time to half life recovery ($t_{1/2}$) between EGFP-B23.1, EGFP-nucleolin, EGFP-fibrillarin and EGFP-PRRSV-N protein.

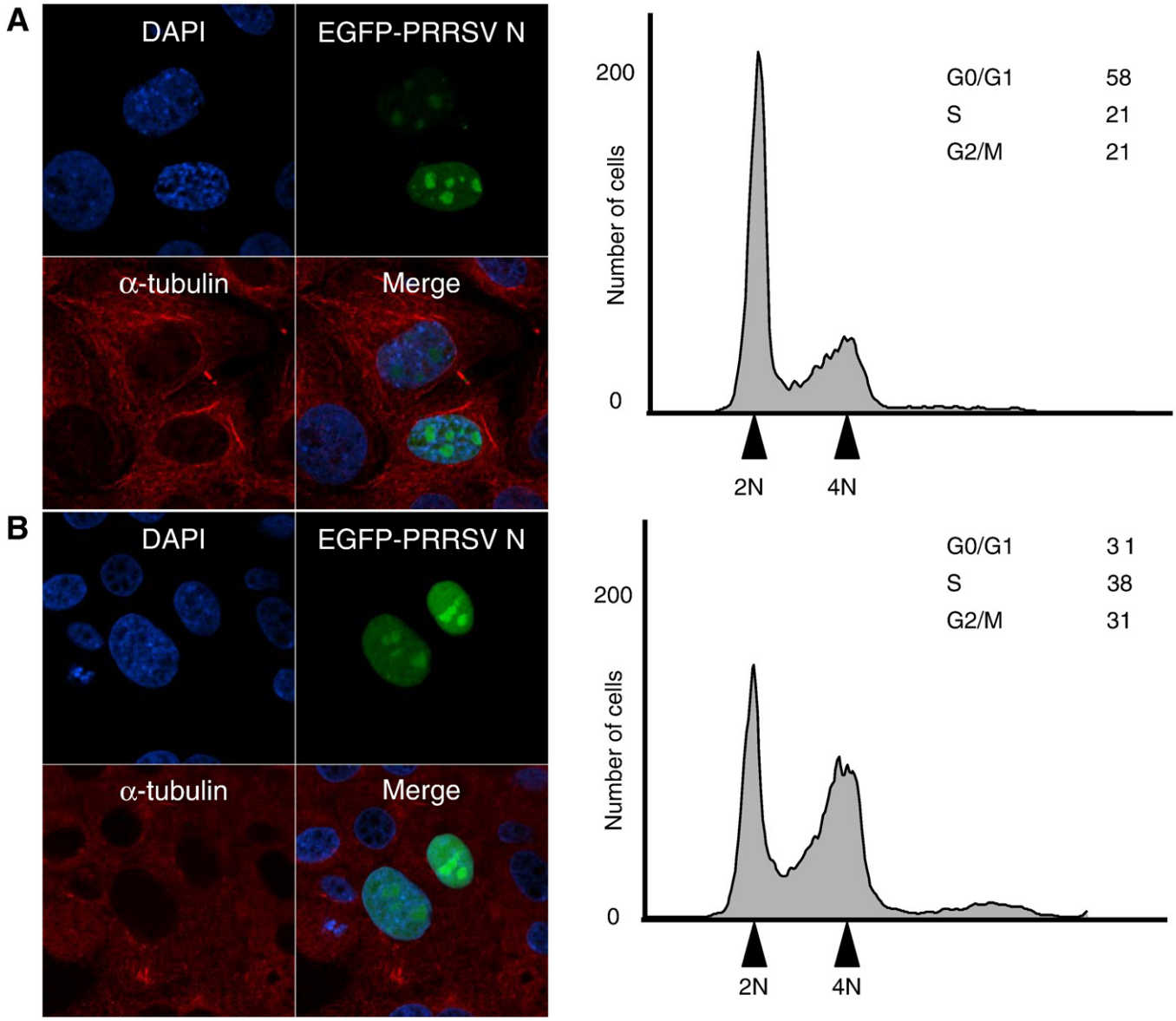

C Trafficking of EGFP-PRRSV N protein from the cytoplasm to the nucleus, nucleolar FLIP with nocodazole

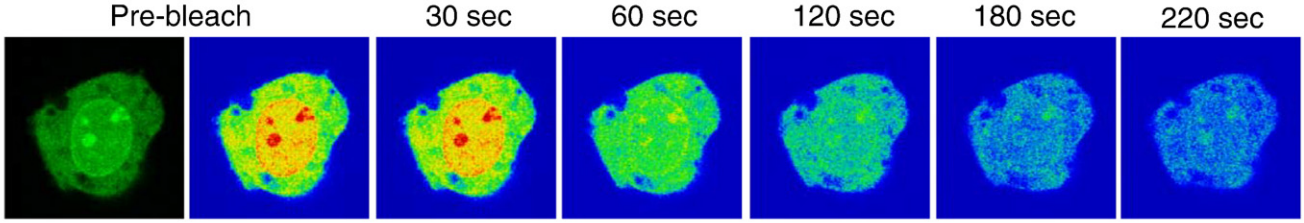

D Trafficking of EGFP-PRRSV N protein from the cytoplasm to the nucleus, nucleolar FLIP at 4°C.

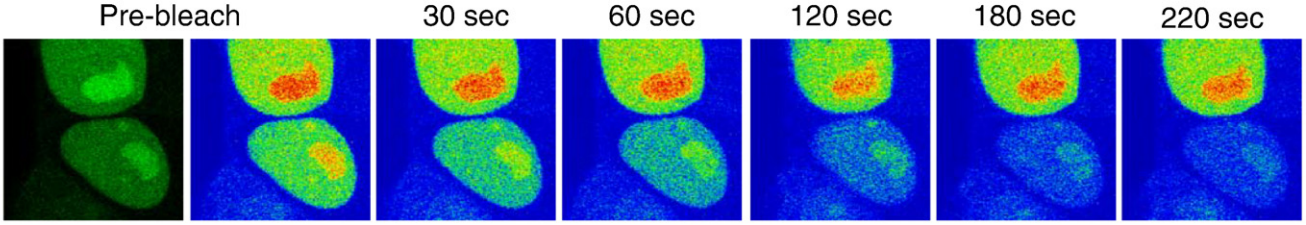

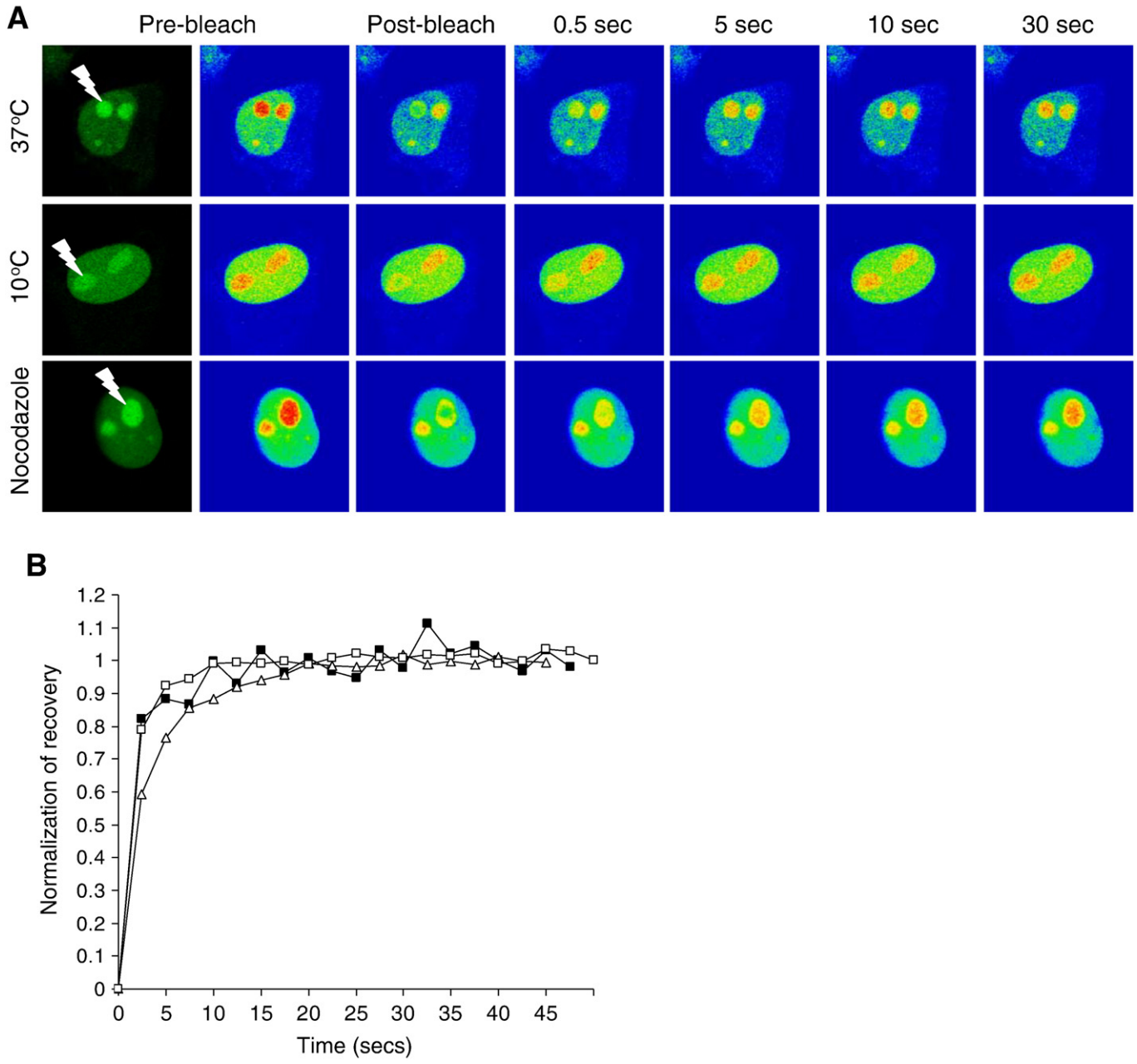

Fig. 4. FRAP analysis of a defined portion of the nucleolus to compare the nucleolar mobility of EGFP-PRRSV-N protein in 3D4/31 cells incubated at 37 °C, 10 °C and at 37 °C in the presence of nocodazole. Presented are the EGFP-protein signals to the left and then the corresponding rainbow image of this where regions of high protein concentration are denoted in red and low to no concentration in blue. The pre- and post-bleach image for each fluorescent fusion protein is presented followed by images sampled at 0.5, 5, 10 and 30 s post-bleach. The width of all images is 35 μm. The position of the photo-bleach on the nucleolus is indicated by the tip of the lighting symbol. (B). Comparison of the normalization of recovery in the photo-bleached area of the nucleolus for EGFP-PRRSV-N protein incubated at 37 °C (□), 10 °C (■) and at 37 °C in the presence of nocodazole (△). The data was processed to ensure that the recovery profiles were set to zero at the initial time point post bleaching, and set to 1 at the final time point.

Expression plasmids

The plasmid pEGFP-PRRSV-N, which expressed PRRSV N protein fused C-terminal to EGFP, was constructed by amplifying the *N* gene using the amplicon FL12 (Truong et al., 2004) (Genbank accession number AY545985) as template. Primers were designed to the 5′ and 3′ end of the *N* gene and contained appropriate restriction enzyme sites; 5′ HindIII and 3′ EcoRI respectively. The amplification product was ligated into the Topo vector pCR2.1 and then cloned into HindIII and EcoRI restricted pEGFP-C2 (Clontech). The insert was sequenced

Fig. 3. A and B. Sub-cellular localisation of EGFP-PRRSV-N protein (green) in 3D4/31 cells which have been either non-treated (A) or treated with nocodazole (B) and fixed and stained for anti-tubulin to highlight microtubules (red) and DAPI to highlight the nucleus (blue). A merged image is also presented. The cell cycle profile of these cells as determined by flow cytometry is also presented to the right with the fluorescent intensities corresponding to a 2N (G0/G1) and 4N (G2/M) DNA content denoted by vertical arrows. The ratio of cells in the G0/G1, S and G2/M phases is provided. (C) and (D) FLIP analysis where when nucleolus is continuously photo-bleached in 3D4/31 cells expressing EGFP-PRRSV-N protein in the presence of nocodazole (C) or incubated at 10 °C (D). Presented are the EGFP-protein signals to the left and then the corresponding rainbow image of this where regions of high protein concentration are denoted in red and low to no concentration in blue. Images were sampled after 10, 30, 60, 120, 180 and 220 s of photo-bleaching.

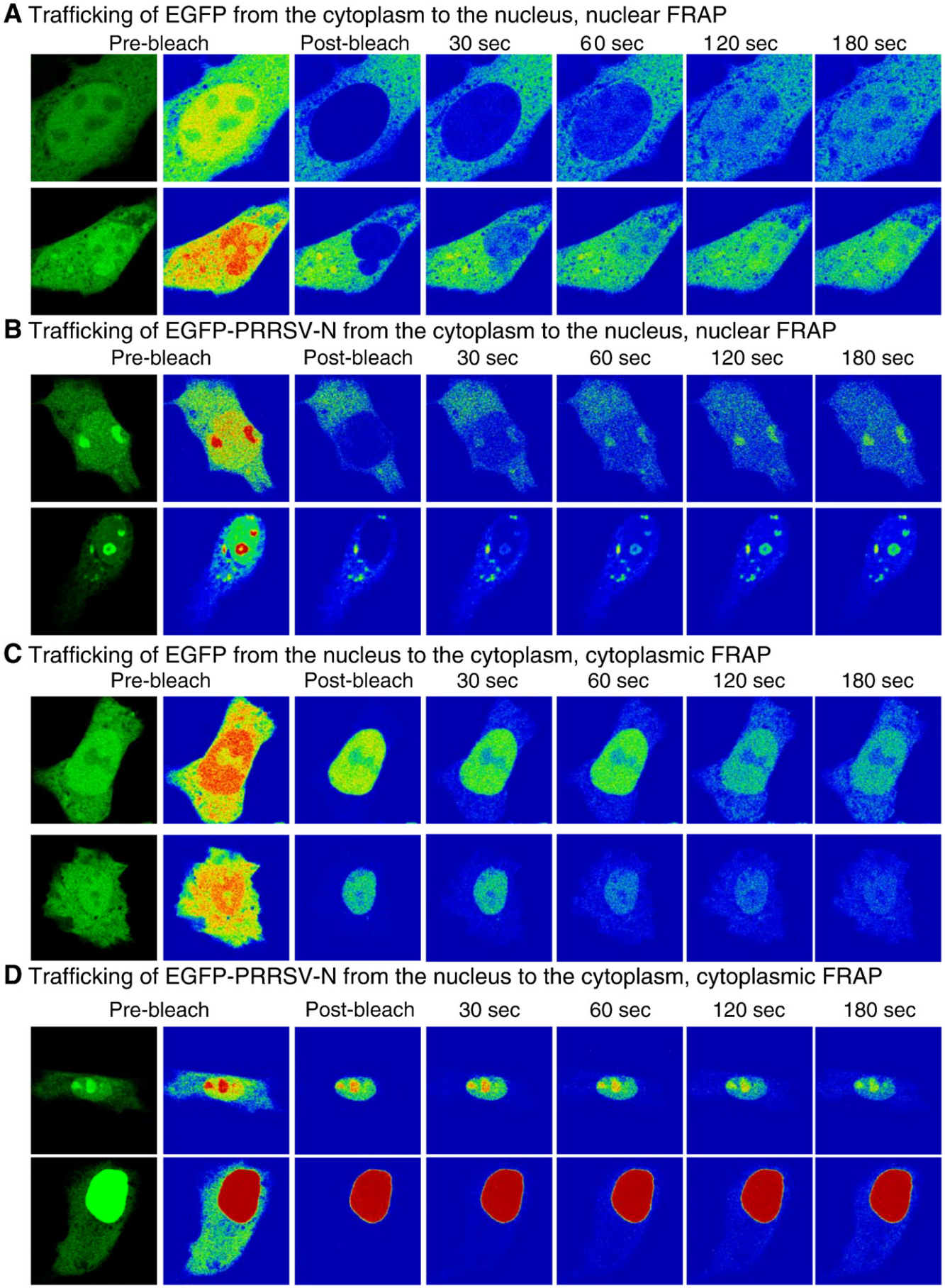
A Trafficking of EGFP from the cytoplasm to the nucleus, nuclear FRAP
Pre-bleach
Post-bleach
30 sec
60 sec
120 sec
180 sec
B Trafficking of EGFP-PRRSV-N from the cytoplasm to the nucleus, nuclear FRAP
Pre-bleach
Post-bleach
30 sec
60 sec
120 sec
180 sec
C Trafficking of EGFP from the nucleus to the cytoplasm, cytoplasmic FRAP
Pre-bleach
Post-bleach
30 sec
60 sec
120 sec
180 sec
D Trafficking of EGFP-PRRSV-N from the nucleus to the cytoplasm, cytoplasmic FRAP
Pre-bleach
Post-bleach
30 sec
60 sec
120 sec
180 sec

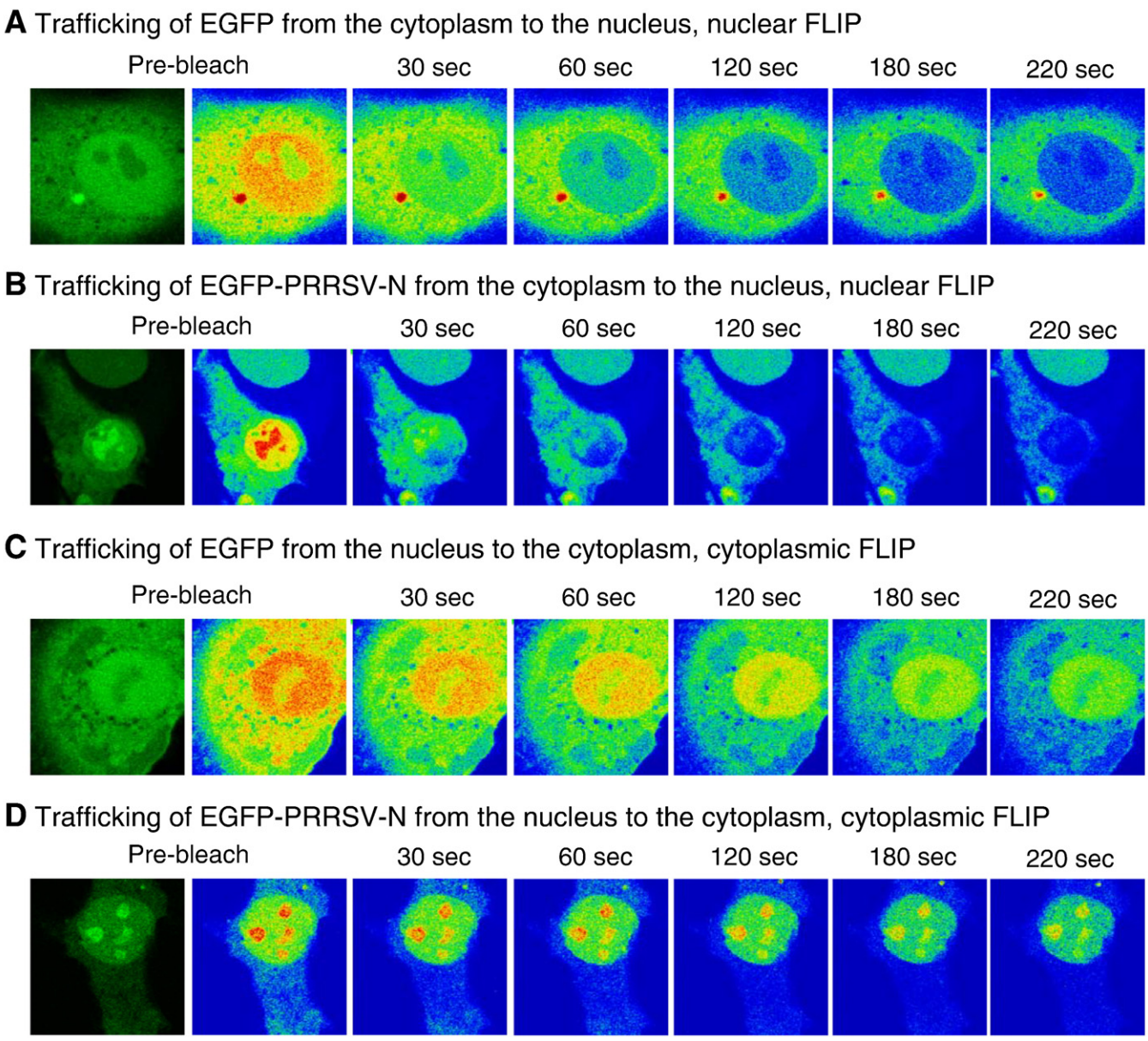

Fig. 6. Trafficking analysis using FLIP of EGFP or EGFP-PRRSV-N protein between the cytoplasm and the nucleus (A and B, respectively) or between the nucleus and the cytoplasm (C and D, respectively) in 3D4/31 cells. Presented are the EGFP-protein signals to the left and then the corresponding rainbow image of this where regions of high protein concentration are denoted in red and low to no concentration in blue. For FLIP pre- and during bleach images are shown and the times indicated (in s) are when the images were sampled. The width of all images is 35 μm.

in both directions to confirm authenticity and western blot analysis to confirm expression. Plasmids which led to the expression of the nucleolar marker proteins EGFP-nucleolin, EGFP-B23.1, DsRed-B23.1 and EFP-fibrillarin have been described previously (Reed et al., 2006; You et al., 2005).

FRAP analysis

Transfected cells were imaged at 37°C in CO_2-independent media (Gibco) supplemented with 5% FBS on an inverted LSM510 META confocal microscope (Carl Zeiss) using a 63× objective and a 4 factor zoom. Five images were captured before a short period of photo-bleaching using conditions that had negligible effects on total cell fluorescence. Photo-bleaching was performed on an area of 12 by 12pixels (approx 20.16μm^2) with a 25mW argon laser at 100% power, bleaching took approximately 1.2s. Fluorescence was analyzed with LSM510 software and raw data was imported into Microsoft Excel for analysis and generation of graphs.

Raw data were averaged before normalizing. Normalization of the data was performed in such a way as to ensure that the recovery profiles were set to zero at the initial time point post bleaching, and set to 1 at the final time point; as previously described (Marcelli et al., 2006; Stenoien et al., 2002). Time to half life recovery ($t_{1/2}$) was performed on the mean raw data, determined by the equation (I_E − I_O) / 2, where I_E was the intensity at the final time point, and I_O the intensity at the time point immediately following photo-bleaching.

Fig. 5. Trafficking analysis of EGFP or EGFP-PRRSV-N protein between the cytoplasm and the nucleus (A and B, respectively) or the nucleus and the cytoplasm (C and D, respectively) using FRAP in 3D4/31 cells. Presented are the EGFP-protein signals to the left and then the corresponding rainbow image of this where regions of high protein concentration are denoted in red and low to no concentration in blue. For FRAP pre- and post-bleach images are shown and the times indicated (in s) are when the images were sampled. The width of all images is 35 μm.

Diffusion coefficient (D) values were calculated from the half life recovery ($t_{1/2}$) using the following diffusion equation $D=(w^2/4_{t_{1/2}})\times 0.88$ where w is the width of the bleach area, approx 1.68μm, and a constant factor of 0.88 was used for a Gaussian beam profile (Axelrod et al., 1976). Data from 5 experiments were used per construct and standard deviation was calculated in the usual manner using Microsoft Excel.

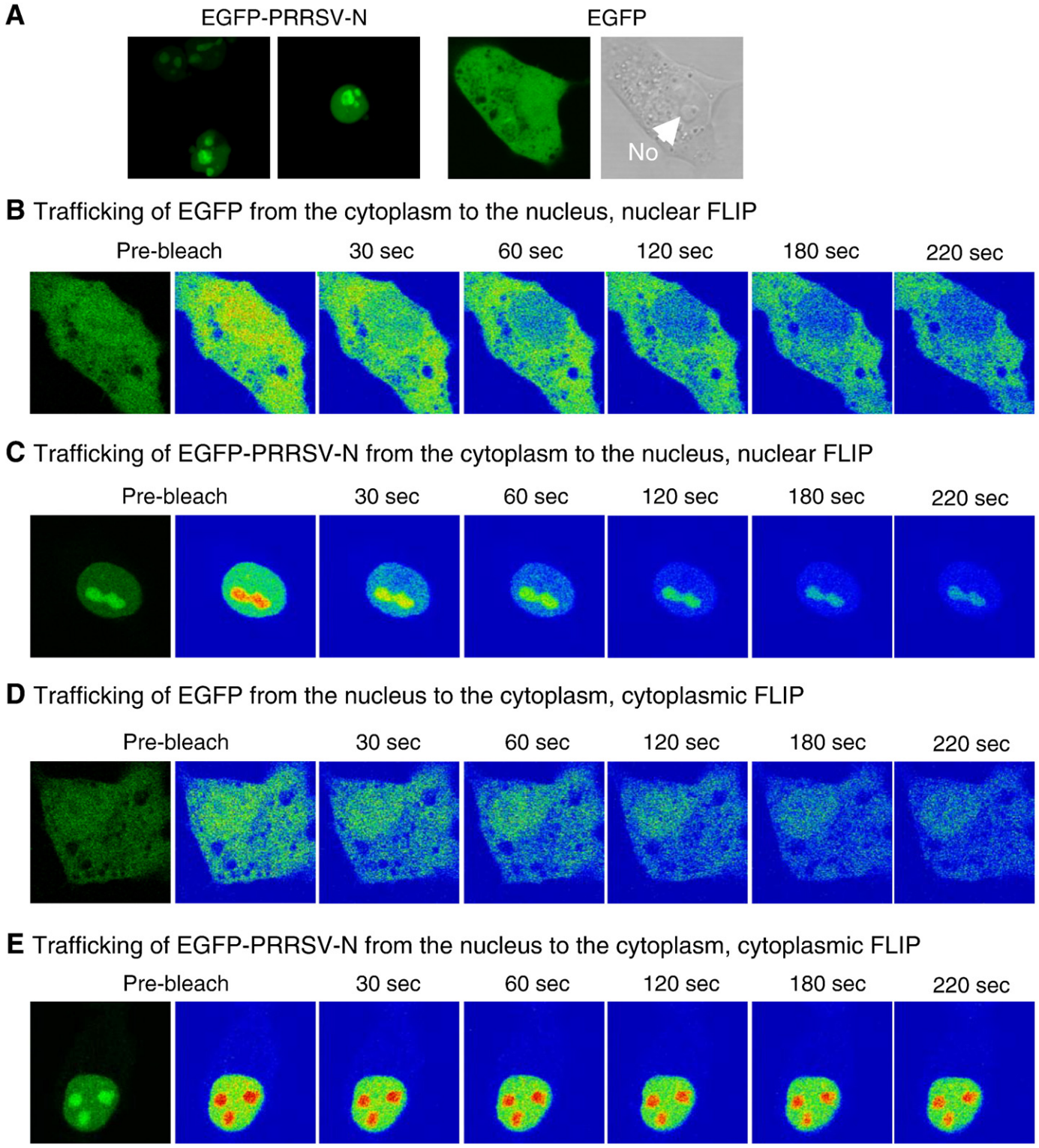

Fig. 7. (A). Live cell confocal analysis of the distribution of EGFP-PRRSV-N protein in MARC-145 cells (two examples shown) compared to EGFP. Note that for EGFP the transmission phase image is presented to show the location of the nucleolus/nucleus and cytoplasm. Trafficking analysis of EGFP or EGFP-PRRSV-N protein between the cytoplasm and the nucleus (B and C, respectively) or between the nucleus and the cytoplasm (D and E, respectively) using FLIP in MARC-145 cells. Presented are the EGFP-protein signals to the left and then the corresponding rainbow image of this where regions of high protein concentration are denoted in red and low to no concentration in blue. For FLIP pre- and during bleach images are shown and the times indicated (in s) are when the images were sampled. The width of all images is 35 μm.

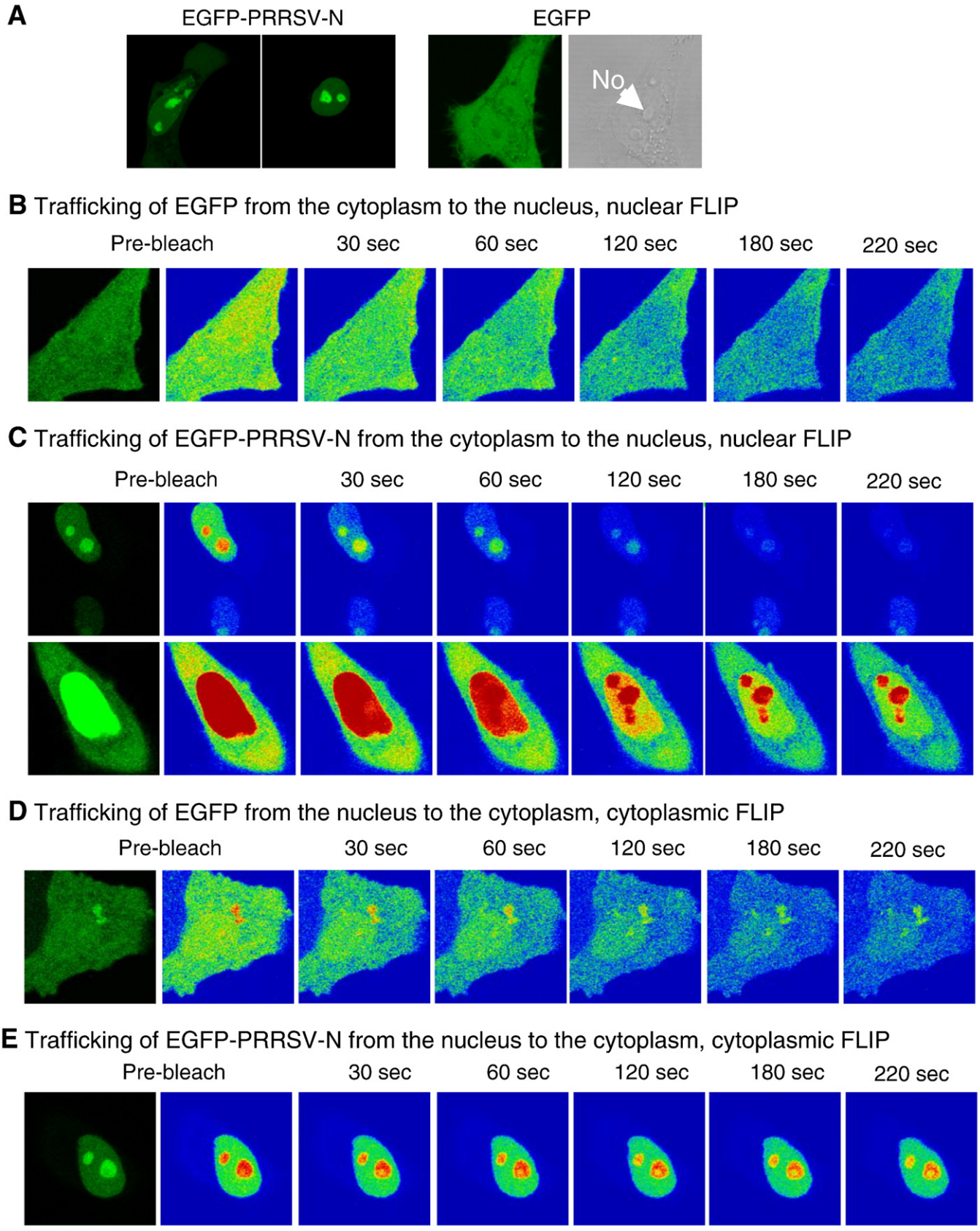

Fig. 8. (A). Live cell confocal analysis of the distribution of EGFP-PRRSV-N protein in HeLa cells (two examples shown) compared to EGFP. Note that for EGFP the transmission phase image is presented to show the location of the nucleolus/nucleus and cytoplasm. Trafficking analysis of EGFP or EGFP-PRRSV-N protein between the cytoplasm and the nucleus (B and C, respectively) or between the nucleus and the cytoplasm (D and E, respectively) using FLIP in MARC-145 cells. Presented are the EGFP-protein signals to the left and then the corresponding rainbow image of this where regions of high protein concentration are denoted in red and low to no concentration in blue. For FLIP pre- and during bleach images are shown and the times indicated (in s) are when the images were sampled. For (C) two examples of lower and higher expression levels are shown in the upper and lower panels, respectively. The width of all images is 35 μm.

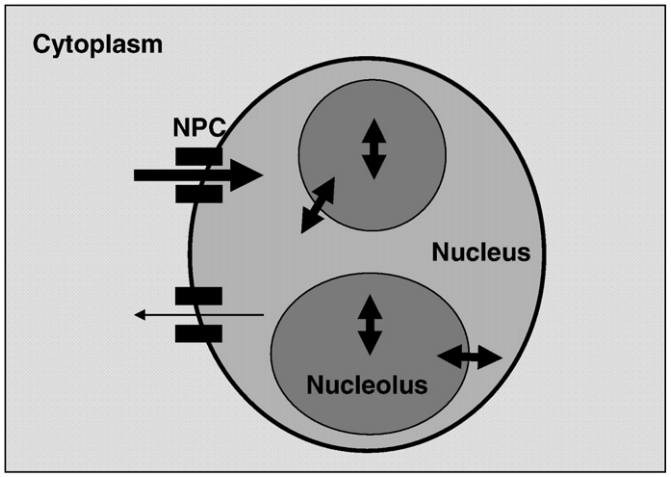

Fig. 9. Model of the trafficking of PRRSV N protein within the cell where the width of arrows denotes the relative movement of N protein and shading is relative concentration of the protein. Trafficking from the cytoplasm to the nucleus and localisation to the nucleolus is fast compared to export of N protein from the nucleus to the cytoplasm which is slower. (NPC denotes nuclear pore complex).

FLIP microscopy

Transfected cells were imaged in glass base dishes as outlined above. Imaging and photo-bleaching was performed with the same laser settings as detailed in the FRAP microscopy. In each FLIP experiment cells were imaged 5 times followed by a period of photo-bleaching for a total time of 3min. Photo-bleaching was performed on a defined area (12 by 12pixels (approx 20.16μm^2)) within the cell for 50 iterations (mean bleach time 2.1s).

Acknowledgments

This research was supported by a National Pork Board grant to JAH. Drs Amanda Stuart and T. David K. Brown at the University of Cambridge are thanked for providing the materials and reagents.

References

Ahlquist, P., 2006. Parallels among positive-strand RNA viruses, reverse-transcribing viruses and double-stranded RNA viruses. Nat. Rev. Microbiol. 4, 371–382.
Andersen, J.S., Lam, Y.W., Leung, A.K., Ong, S.E., Lyon, C.E., Lamond, A.I., Mann, M., 2005. Nucleolar proteome dynamics. Nature 433, 77–83.
Andersen, J.S., Lyon, C.E., Fox, A.H., Leung, A.K.L., Lam, Y.W., Steen, H., Mann, M., Lamond, A.I., 2002. Directed proteomic analysis of the human nucleolus. Curr. Biol. 12, 1–11.
Axelrod, D., Koppel, D.E., Schlessinger, J., Elson, E., Webb, W.W., 1976. Mobility measurement by analysis of fluorescence photobleaching recovery kinetics. Biophys. J. 16, 1055–1069.
Boisvert, F.M., van Koningsbruggen, S., Navascues, J., Lamond, A.I., 2007. The multifunctional nucleolus. Nat. Rev., Mol. Cell Biol. 8, 574–585.
Cawood, R., Harrison, S.M., Dove, B.K., Reed, M.L., Hiscox, J.A., 2007. Cell cycle dependent localisation of the coronavirus nucleocapsid protein. Cell Cycle 6, 863–867.
Chu, J.J., Ng, M.L., 2002. Trafficking mechanism of West Nile (Sarafend) virus structural proteins. J. Med. Virol. 67, 127–136.
Das, S.C., Nayak, D., Zhou, Y., Pattnaik, A.K., 2006. Visualization of intracellular transport of vesicular stomatitis virus nucleocapsids in living cells. J. Virol. 80, 6368–6377.
de Haan, C.A., Reggiori, F., 2008. Are nidoviruses hijacking the autophagy machinery? Autophagy 4, 276–279.
Dove, B., Brooks, G., Bicknell, K., Wurm, T., Hiscox, J.A., 2006. Cell cycle perturbations induced by infection with the coronavirus infectious bronchitis virus and their effect on virus replication. J. Virol. 80, 4147–4156.
Harrison, S.M., Dove, B.K., Rothwell, L., Kaiser, P., Tarpey, I., Brooks, G., Hiscox, J.A., 2007. Characterisation of cyclin D1 down-regulation in coronavirus infected cells. FEBS Lett. 581, 1275–1286.
Hernandez-Verdun, D., 2006. Nucleolus: from structure to dynamics. Histochem. Cell Biol. 125, 127–137.
Hernandez-Verdun, D., Roussel, P., 2003. Regulators of nucleolar functions. Prog. Cell Cycle Res. 5, 301–308.
Hiscox, J.A., 2002. Brief review: the nucleolus — a gateway to viral infection? Arch. Virol. 147, 1077–1089.
Hiscox, J.A., 2003. The interaction of animal cytoplasmic RNA viruses with the nucleus to facilitate replication. Virus Res. 95, 13–22.
Hiscox, J.A., 2007. RNA viruses: hijacking the dynamic nucleolus. Nat. Rev. Microbiol. 5, 119–127.
Hiscox, J.A., Wurm, T., Wilson, L., Cavanagh, D., Britton, P., Brooks, G., 2001. The coronavirus infectious bronchitis virus nucleoprotein localizes to the nucleolus. J. Virol. 75, 506–512.
Kim, H.S., Kwang, J., Yoon, I.J., Joo, H.S., Frey, M.L., 1993. Enhanced replication of porcine reproductive and respiratory syndrome (PRRS) virus in a homogeneous subpopulation of MA-104 cell line. Arch. Virol. 133, 477–483.
Kim, S.H., Macfarlane, S., Kalinina, N.O., Rakitina, D.V., Ryabov, E.V., Gillespie, T., Haupt, S., Brown, J.W., Taliansky, M., 2007a. Interaction of a plant virus-encoded protein with the major nucleolar protein fibrillarin is required for systemic virus infection. Proc. Natl. Acad. Sci. U. S. A. 104, 11115–11120.
Kim, S.H., Ryabov, E.V., Kalinina, N.O., Rakitina, D.V., Gillespie, T., MacFarlane, S., Haupt, S., Brown, J.W., Taliansky, M., 2007b. Cajal bodies and the nucleolus are required for a plant virus systemic infection. EMBO J. 26, 2169–2179.
Lee, C., Hodgins, D., Calvert, J.G., Welch, S.K., Jolie, R., Yoo, D., 2006. Mutations within the nuclear localization signal of the porcine reproductive and respiratory syndrome virus nucleocapsid protein attenuate virus replication. Virology 346, 238–250.
Leung, A.K., Trinkle-Mulcahy, L., Lam, Y.W., Andersen, J.S., Mann, M., Lamond, A.I., 2006. NOPdb: nucleolar proteome database. Nucleic Acids Res. 34, D218–D220.
Li, F.Q., Xiao, H., Tam, J.P., Liu, D.X., 2005. Sumoylation of the nucleocapsid protein of severe acute respiratory syndrome coronavirus. FEBS Lett. 579, 2387–2396.
Li, F.Q., Tam, J.P., Liu, D.X., 2007. Cell cycle arrest and apoptosis induced by the coronavirus infectious bronchitis virus in the absence of p53. Virology 365, 435–445.
Macara, I.G., 2001. Transport into and out of the nucleus. Microbiol. Mol. Biol. Rev. 65, 570–594.
Marcelli, M., Stenoien, D.L., Szafran, A.T., Simeoni, S., Agoulnik, I.U., Weigel, N.L., Moran, T., Mikic, I., Price, J.H., Mancini, M.A., 2006. Quantifying effects of ligands on androgen receptor nuclear translocation, intranuclear dynamics, and solubility. J. Cell. Biochem. 98, 770–788.
Matthews, D.A., Olson, M.O., 2006. What is new in the nucleolus? Workshop on the nucleolus: new perspectives. EMBO Rep. 7, 870–873.
Mayer, C., Grummt, I., 2005. Cellular stress and nucleolar function. Cell Cycle. 4, 1036–1038.
Misteli, T., 2001. Protein dynamics: implications for nuclear architecture and gene expression. Science 291, 843–847.
Ning, B., Shih, C., 2004. Nucleolar localization of human hepatitis B virus capsid protein. J. Virol. 78, 13653–13668.
Pei, Y., Hodgins, D.C., Lee, C., Calvert, J.G., Welch, S.K., Jolie, R., Keith, M., Yoo, D., 2008. Functional mapping of the porcine reproductive and respiratory syndrome virus capsid protein nuclear localization signal and its pathogenic association. Virus Res. 135, 107–114.
Phair, R.D., Misteli, T., 2000. High mobility of proteins in the mammalian cell nucleus. Nature. 404, 604–609.
Posthuma, C.C., Pedersen, K.W., Lu, Z., Joosten, R.G., Roos, N., Zevenhoven-Dobbe, J.C., Snijder, E.J., 2008. Formation of the arterivirus replication/transcription complex: a key role for nonstructural protein 3 in the remodeling of intracellular membranes. J. Virol. 82, 4480–4491.
Ramanathan, H.N., Chung, D.H., Plane, S.J., Sztul, E., Chu, Y.K., Guttieri, M.C., McDowell, M., Ali, G., Jonsson, C.B., 2007. Dynein-dependent transport of the hantaan virus nucleocapsid protein to the endoplasmic reticulum-Golgi intermediate compartment. J. Virol. 81, 8634–8647.
Reed, M.L., Dove, B.K., Jackson, R.M., Collins, R., Brooks, G., Hiscox, J.A., 2006. Delineation and modelling of a nucleolar retention signal in the coronavirus nucleocapsid protein. Traffic 7, 833–848.
Reed, M.L., Howell, G., Harrison, S.M., Spencer, K.A., Hiscox, J.A., 2007. Characterization of the nuclear export signal in the coronavirus infectious bronchitis virus nucleocapsid protein. J. Virol. 81, 4298–4304.
Rowland, R.R.R., Yoo, D., 2003. Nucleolar-cytoplasmic shuttling of PRRSV nucleocapsid protein: a simple case of molecular mimicry or the complex regulation by nuclear import, nucleolar localization and nuclear export signal sequences. Virus Res. 95, 23–33.
Rowland, R.R., Kerwin, R., Kuckleburg, C., Sperlich, A., Benfield, D.A., 1999. The localisation of porcine reproductive and respiratory syndrome virus nucleocapsid protein to the nucleolus of infected cells and identification of a potential nucleolar localization signal sequence. Virus Res. 64, 1–12.
Rowland, R.R.R., Schneider, P., Fang, Y., Wootton, S., Yoo, D., Benfield, D.A., 2003. Peptide domains involved in the localization of the porcine reproductive and respiratory syndrome virus nucleocapsid protein to the nucleolus. Virology 316, 135–145.
Rowland, R.R., Chauhan, V., Fang, Y., Pekosz, A., Kerrigan, M., Burton, M.D., 2005. Intracellular localization of the severe acute respiratory syndrome coronavirus nucleocapsid protein: absence of nucleolar accumulation during infection and after expression as a recombinant protein in Vero cells. J. Virol. 79, 11507–11512.
Rubbi, C.P., Milner, J., 2003. Disruption of the nucleolus mediates stabilization of p53 in response to DNA damage and other stresses. EMBO J. 22, 6068–6077.
Stenoien, D.L., Mielke, M., Mancini, M.A., 2002. Intranuclear ataxin1 inclusions contain both fast- and slow-exchanging components. Nat. Cell Biol. 4, 806–810.
Taylor, M.P., Kirkegaard, K., 2008. Potential subversion of autophagosomal pathway by picornaviruses. Autophagy 4, 286–289.
Terry, L.J., Shows, E.B., Wente, S.R., 2007. Crossing the nuclear envelope: hierarchical regulation of nucleocytoplasmic transport. Science. 318, 1412–1416.
Tijms, M.A., van der Meer, Y., Snijder, E.J., 2002. Nuclear localization of non-structural protein 1 and nucleocapsid protein of equine arteritis virus. J. Gen. Virol. 83, 795–800.

Timani, K.A., Liao, Q., Ye, L., Zeng, Y., Liu, J., Zheng, Y., Yang, X., Lingbao, K., Gao, J., Zhu, Y., 2005. Nuclear/nucleolar localization properties of C-terminal nucleocapsid protein of SARS coronavirus. Virus Res. 114, 23–34.

Truong, H.M., Lu, Z., Kutish, G.F., Galeota, J., Osorio, F.A., Pattnaik, A.K., 2004. A highly pathogenic porcine reproductive and respiratory syndrome virus generated from an infectious cDNA clone retains the in vivo virulence and transmissibility properties of the parental virus. Virology. 325, 308–319.

Uchil, P.D., Kumar, A.V., Satchidanandam, V., 2006. Nuclear localization of flavivirus RNA synthesis in infected cells. J Virol. 80, 5451–5464.

van Hemert, M.J., de Wilde, A.H., Gorbalenya, A.E., Snijder, E.J., in press. The in vitro RNA synthesizing activity of the isolated arterivirus replication/transcription complex is dependent on a host factor. J. Biol. Chem. doi:10.1074/jbc.M708136200.

Weidman, M.K., Sharma, R., Raychaudhuri, S., Kundu, P., Tsai, W., Dasgupta, A., 2003. The interaction of cytoplasmic RNA viruses with the nucleus. Virus Res. 95, 75–85.

Weingartl, H.M., Sabara, M., Pasick, J., van Moorlehem, E., Babiuk, L., 2002. Continuous porcine cell lines developed from alveolar macrophages: partial characterization and virus susceptibility. J. Virol. Methods 104, 203–216.

Whittaker, G.R., Kann, M., Helenius, A., 2000. Viral entry into the nucleus. Annu. Rev. Cell Dev. Biol. 16, 627–651.

Wills, R.W., Doster, A.R., Galeota, J.A., Sur, J.-H., Osorio, F.A., 2003. Duration of infection and proportion of pigs persistently infected with porcine reproductive and respiratory syndrome virus. J. Clin. Microbiol. 41, 58–62.

Wurm, T., Chen, H., Britton, P., Brooks, G., Hiscox, J.A., 2001. Localisation to the nucleolus is a common feature of coronavirus nucleoproteins and the protein may disrupt host cell division. J. Virol. 75, 9345–9356.

Yoo, D., Wootton, S.K., Li, G., Song, C., Rowland, R.R., 2003. Colocalization and interaction of the porcine arterivirus nucleocapsid protein with the small nucleolar RNA-associated protein fibrillarin. J. Virol. 77, 12173–12183.

You, J., Dove, B.K., Enjuanes, L., DeDiego, M.L., Alvarez, E., Howell, G., Heinen, P., Zambon, M., Hiscox, J.A., 2005. Subcellular localization of the severe acute respiratory syndrome coronavirus nucleocapsid protein. J. Gen. Virol. 86, 3303–3310.

You, J.H., Reed, M.L., Hiscox, J.A., 2007. Trafficking motifs in the SARS-coronavirus nucleocapsid protein. Biochem. Biophys. Res. Commun. 358, 1015–1020.